

Synthesis and Characterization of Hydrophilic High Glycolic Acid–Poly(DL-Lactic-co-Glycolic Acid)/ Polycaprolactam/Polyvinyl Alcohol Blends and Their Biomedical Application as a Ureteral Material

Venkatesan Nandakumar,[†] Ganesan Suresh,[†] Samuel Chittaranjan,[‡] and Mukesh Doble^{*,†}

[†]Department of Biotechnology, Indian Institute of Technology Madras, Chennai, India

[‡]Department of Orthopedics, CMC Hospital, Vellore, India

S Supporting Information

ABSTRACT: Synthesis of low molecular weight poly(DL-lactic-co-glycolic acid), homopolymer poly lactic acid (PLA), and formulation of a hydrophilic blend with polycaprolactam and polyvinyl alcohol is reported. The surface properties and the morphology of the blends were characterized with a goniometer and scanning electron microscopy (SEM). The mechanical property was analyzed with a tensile strength analyzer. The composition of these blends was verified by Fourier transform infrared (FTIR), ¹H, and ¹³C NMR spectroscopy. The biocompatibility and hemocompatibility and the extent of salt encrustation and adhesion of virulent bacterial strains on the blends were also investigated. All the blends were biocompatible and hemocompatible. Adhesion of virulent *E. coli* was high with blood plasma protein pretreated blends than *P. mirabilis*. The pattern of encrustation of Ca, Mg, and P was similar on all the blends with calcium being the predominant encrustant. After 3 weeks, 3–10% weight loss was observed with maximum weight loss observed in the poly(lactic-co-glycolic acid) 10:90 based blend. The PLA based blend dominates all the other blends in all the aspects tested.

1. INTRODUCTION

Ureteral stents are widely used to facilitate the flow of urine from the renal pelvis to the bladder and maintain open state of the ureter. They also find use in most of the urogenetic disorders including primary or malignant carcinomas, obstructive uropathy, ureteric injury, radiation fibrosis, or retroperitoneal fibrosis.¹ The duration of a ureteral stent in a patient is dependent on the clinical condition and may vary from a few days to months. The prolonged indwelling time and proper functioning of the synthetic material as a ureteral stent is hindered by two main factors namely salt encrustation and biofilm formation.² Silicone, polyurethane, and polyurethane based polymers are widely used as stent material.² Although polyurethane is more widely used than other materials owing to its good biocompatibility, the above-mentioned issues still hinder its prolonged indwelling time. To date, no material is totally inert within the urinary environment. These polymers are good substrates for the adhesion of urine components, in particular urinary salts. They also favor the adhesion of uropathogens which over a period of time develop into a three-dimensional structure termed as biofilm.² Although bacterial adhesion is attributed to the deposition of organic matrix, increased protein adhesion on the material is attributed to the surface properties of the latter. Development of this organic matrix³ on the polymer surface can bind ions, aggregate crystals, and also favor bacterial attachment which in turn leads to further encrustation.

Surface properties that play a key role in reducing bacterial adhesion and formation of biofilm include hydrophilicity, steric hindrance, surface roughness, and the type of conditioning layer.⁴ The type of conditioning layer formed in turn depends on the surface properties of the polymer in particular

electrostatic and hydrophobic interactions between the polymer surface and the protein.⁵ Hydrophobicity is considered as an important parameter which affects bacterial adhesion, but the exact role of surface hydrophobicity is not well established with different bacterial strains and environment.

Degradation of the stent inside the human body with time is desired since it can obviate the need for another surgery to remove it after the treatment period. Stent fracture and breakage are other complications which can arise due to the encrustation and biofilm formation on the stent surface. This makes the removal process more complicated.² The currently available materials do not degrade.

Hence, this research is focused toward design of novel biodegradable polymers as ureteral stent materials. Homopolymer including polylactic acid (PLA) and polyglycolic acid (PGA) are widely tested for their use as stents. They are biodegradable and biocompatible, but lack of sufficient mechanical strength results in their uneven fragmentation resulting in vesico-ureteric reflux.⁶ Studies with PLA have shown that bacterial adherence depends on the type of bacteria.⁷ Whereas, in the case of PGA both encrustation and bacterial adhesion is minimal in spite of its fragility.² The self-reinforced poly(lactic-co-glycolic acid) (PLGA) stent is found to exhibit superior drainage (complete removal of urine) and better antireflux properties than other materials.⁸ The degradation pattern of PLGA is more uniform, and it is more biocompatible than metallic stents.⁹ It is also used as a partial

Received: August 20, 2012

Revised: November 14, 2012

Accepted: December 12, 2012

Published: December 12, 2012

internal catheter in ureteropelvic junction.¹⁰ The mode of degradation of PLGA polymers is mainly by hydration, followed by chain scission. The rate of degradation is multifactorial, and it depends on monomer ratio, molecular weight, pH, and the environment in which it is located.

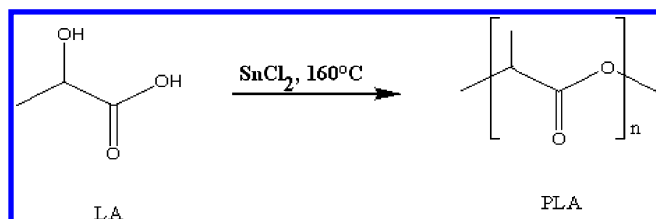
In light of this, the present study is aimed at designing novel hydrophilic high glycolic acid–poly(DL-lactic-co-glycolic acid)/polycaprolactam/polyvinyl alcohol blends with good mechanical strength and testing their performance in vitro as ureteral stent material. Polycaprolactam is chosen for various reasons. Primarily it is biodegradable and biocompatible and has high tensile strength. In the current study, it is mainly used to increase the mechanical strength of the blend, since PLGA has poor mechanical properties. Polyvinyl alcohol is chosen to increase the hydrophilicity, since it is known that the presence of hydrophilic passivating groups discourage bacterial adhesion.⁴ *E. coli*¹¹ and *P. mirabilis*¹² are selected for bacterial adhesion studies, because the former is a common uropathogen and the latter is a urease positive strain which increases the alkalinity of the solution thereby enhancing encrustation. The biocompatibility of these blends in the presence of myoblasts cells, whole blood, and platelets is also studied.

2. MATERIALS AND EXPERIMENTAL METHODS

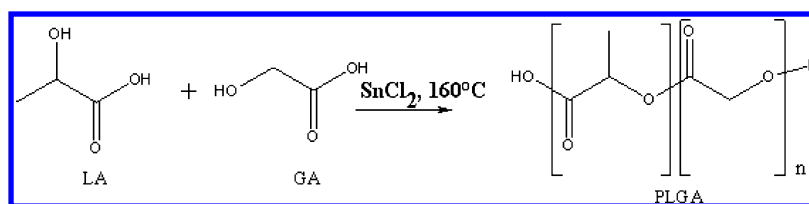
DL-Lactic acid (LA) and DL-glycolic acid (GA) were purchased from Fischer scientific (India). Polycaprolactam (PCPL) and polyvinyl alcohol (PVA) were purchased from Sigma (India). Sodium sulfate, sodium phosphate, sodium dihydrogen phosphate, sodium citrate, sodium oxalate, calcium chloride, magnesium sulfate hepta-hydrate, ammonium chloride, and urea were purchased from Merck, India. Bovine serum albumin (BSA), nutrient agar, nutrient broth, Dulbecco's modified eagle medium (DMEM), and antibiotics were purchased from Himedia, India. Fetal bovine serum albumin (FBS) from Invitrogen and L6-myoblast cells were purchased from NCCS, India. Clinical strains of *E. coli* and *P. mirabilis* (source of isolation: urine culture) were obtained from SRM Dental College, Chennai, India

2.1. Synthesis of PLGA. Synthesis of low molecular weight homopolymer, PLA, and copolymer, PLGA, was carried out according to an earlier reported method with some modifications.¹³ Scheme 1 represents the synthesis of PLA

Scheme 1. Synthesis of Homopolymer Polylactic Acid (PLA)



Scheme 2. Synthesis of Copolymer Poly(Lactic-co-Glycolic Acid) (PLGA)



from its monomer DL-lactic acid, and Scheme 2 represents synthesis of PLGA from its monomers DL-lactic acid and DL-glycolic acid. Predetermined molar ratios of DL-lactic and glycolic acid with stannous chloride (SnCl_2) were taken in a round bottomed flask immersed in an oil bath which was maintained at 160 °C under pressure and continuous stirring for 48 h. The polymerized polyesters were purified by chloroform/ether precipitation and dried in a vacuum oven at room temperature.

Preparation of Polymer Blend. A solvent cast-evaporation method was used to prepare films of polymer blends.¹ PLGA was blended with PCPL in the ratio of 50/50 (w/w %) and dissolved in 25 mL tetrahydrofuran containing 4% v/v trifluoroacetic acid at room temperature. The polymer solution was then added to 0.3% PVA solution. The resulting polymer aggregate was filtered under vacuum and redissolved in tetrahydrofuran containing 4% v/v trifluoroacetic acid. The solution was then cast on a petridish, and the solvent was slowly evaporated and vacuum-dried in an oven at 37 °C for 24 h, leaving a thin film of the blend. The cast film was cut into 1 cm × 1 cm dimension and stored at 4 °C until further studies.

2.2. Characterization of Blends. The blends were characterized using different analytical tools.¹⁴ The infrared spectrum of the polymer blend was recorded in the range of 400–4000 cm^{-1} in transmittance mode with an accuracy of 4 cm^{-1} with an FTIR (FT-IR 4100, Jasco). ¹H NMR and ¹³C NMR spectra were recorded with Bruker 500 MHz NMR, and the chemical shift was measured in parts per million with tetramethylsilane as internal standard. DSC measurements were carried out on Netzsch DSC 204 differential scanning calorimeter under nitrogen atmosphere at a constant heating rate of 10 °C/min from 25 to 500 °C. Thermogravimetric analysis was carried out at a heating rate of 10 °C/min from 25 to 500 °C under nitrogen atmosphere on TGA Q500 V20.10 Universal TA Instruments. The number and weight average molecular weight and its distribution were determined by an Agilent 1100 series high-performance liquid chromatography (India). PLgel Colum-PL mixed B (Polymer laboratories, UK) was used with tetrahydrofuran as the solvent and polystyrene (Easical, Polymer laboratories, UK) as the internal standard at a flow rate of 1 mL/min at 35 °C. Surface hydrophilicity of the polymer film was determined by placing a drop of ultrapure water on it and measuring the contact angle using a Goniometer (Kruss contact angle, Germany). The tensile strength analysis of the blends was analyzed with the help of Instron-3367 (USA). The samples were prepared as per ASTM D882-12 standards.

2.3. Biological Characterization of Blends. **2.3.1. In vitro Biocompatibility of L6 Myoblasts Cells. Cell Line and Culture Medium.** L6 myoblasts, derived from skeletal muscles of rat, was maintained in Dulbecco's modified eagle medium with 10% fetal bovine serum supplemented with penicillin (120 units/mL), streptomycin (75 mg/mL), gentamycin (160 mg/

mL), and amphotericin B (3 mg/mL) at 37 °C and humidified with 5% CO₂. Cells were cultured until they reached confluence and the analysis was carried out with cells after 10–15 passages.

Polymer films of dimension 1 cm × 1 cm were initially kept immersed in 70% ethanol for an hour for sterilization and kept immersed in phosphate buffer solution (PBS, pH of 7.2) for 24 h in a 24 well plate. L6 cells were seeded on to the films with an inoculum dosage of 1 × 10⁴ cells/well and incubated for 24 and 48 h. The viable cells on the surface of the film were quantified with MTT assay.¹⁵ Simultaneously, cells were cultured with DiI, a live cell stain, washed twice with PBS (pH 7.4), then seeded on the films and incubated for 24 and 48 h. The viability of these cells was visualized using a confocal laser scanning microscope (Nikon A1/LSM 510, Zeiss)

2.3.2. In vitro Hemocompatibility Analysis. Platelet Adhesion Assay. Adhesion of platelet on the film was determined using a method reported earlier¹⁶ with platelet rich plasma obtained from heparinized blood from a healthy volunteer. Films were sterilized with ethanol and equilibrated with PBS for 24 h. They were then incubated with platelet rich plasma with a cell count of 2 × 10⁵ cells/well for 2 h at 37 °C and humidified with 5% CO₂. The films were fixed with 1.5% glutaraldehyde, dehydrated with series of ethanol–water solutions (50, 60, 70, 80, 90, 100% v/v) and visualized under a scanning electron microscope (FEI Quanta 200, USA) after coating with gold.

Whole Blood Analysis. Compatibility of blends with whole blood¹⁶ was determined using a heparinized whole blood from a healthy volunteer. Ethanol sterilized films were equilibrated with PBS (pH 7.2) for 24 h followed by incubation with whole blood for 24 h. Then they were fixed with 1.5% glutaraldehyde and dehydrated with series of ethanol–water solutions and visualized under a scanning electron microscope after coating with gold.

2.3.3. Application of Blends As Ureteral Stents. Encrustation Analysis. Rate of encrustation of salts on the films was determined with artificial urine.¹ The experiments were carried out in McCartney bottles, with few modifications to the method reported earlier.¹ Films of dimension 1 cm × 1 cm were incubated with artificial urine (S22) under aseptic conditions, under constant shaking at 200 rpm and 37 °C for 3 weeks.

The films were removed every week and the salts adhered were dislodged by low frequency water bath sonication. The encrustants were dissolved with 5% (v/v) hydrochloric acid. The samples were digested in a microwave oven, and the concentration of calcium, magnesium, and phosphorus were determined with the help of inductively coupled plasma–optical emission spectrometer (Perkin-Elmer-Optima 5300 DV ICP–OES).

Bacterial Adhesion Assay. The adhesion of clinical isolates, Gram negative *E. coli* and *P. mirabilis*, was determined on the films surface pretreated with human blood plasma. Films were equilibrated with PBS (pH 7.2) for 24 h and exposed to blood plasma for 2 h at 37 °C. Then, they were washed thrice with PBS. The films treated with PBS alone were taken as control. The films were then incubated with 0.5 OD of the bacterial cell suspension in PBS for 2.5 h at 37 °C.¹⁷

After incubation, each film was transferred to a sterile container containing saline and the adherent bacteria was dislodged with the help of a low frequency water bath sonicator for 30 s. The number of viable bacteria was calculated as colony-forming units (CFU).¹ Simultaneously, the films were

also fixed with glutaraldehyde, dehydrated, and visualized under a scanning electron microscope.

2.4. Degradation Studies. Preweighed films were incubated in artificial urine (pH 6) at 37 °C, and they were removed every week for 3 weeks. Then they were freeze-dried for 24 h, and their weights were measured.¹⁸ The percentage weight loss is given as

$$\% = (W_i - W_t/W_i) * 100$$

Where W_i is the initial dry weight of the film, and W_t is the dry weight of the film at different time periods.

2.5. Statistical Analysis. All the experiments were repeated thrice. Two sample *t* test and one way ANOVA were performed with the help of Minitab 14 (Minitab Inc. USA) to determine the statistical significance of the results. A *p* value less than 0.05 is considered as statistically significant.

3. RESULT

3.1. Characterization of Homopolymer PLA and Copolymer PLGA. The molar ratios of the synthesized homopolymer, PLA, and copolymer, PLGA, were determined from the ¹H and ¹³C NMR spectra (S1–S8 Supporting Information) and listed in Table I. The chemical shift values

Table I. Characteristics of PLA and PLGA

| polymer | feed ratio ^a LA:GA | ¹ H NMR ^b | molecular weight ^c (g/mol) M_w | T_g^d (°C) | contact angle (°) |
|---------------|----------------------------------|---------------------------------|---|-----------------|-------------------|
| PLA | 100:0 | | 8700 | 38.73 | 77 ± 0.9 |
| PLGA 40:60 | 40:60 | 43.85:56.15 | 9100 | 45.73 | 62.2 ± 0.66 |
| PLGA 20:80 | 20:80 | 19.28:80.72 | 7505 | 45.73 | 59 ± 0.21 |
| PLGA 10:90 | 10:90 | 8.18:91.82 | 8200 | 49.73 | 51 ± 0.46 |

^aCalculated from monomer feed ratios. ^bCalculated from proton NMR spectra. ^cObtained from GPC curves M_w weight average molecular weight. ^dMidpoint of DSC glass transition curve.

estimated from NMR data for PLA are as follows: ¹H NMR (500 MHz, CDCl₃, δ) 2.19 (CH₃), 4.41 (CH₂), 5.20 (CH); ¹³C NMR (125 MHz, CDCl₃, δ) 66.50 (CH₂), 208.84 (CO). Chemical shift values for PLGA 40:60 are ¹H NMR (500 MHz, CDCl₃ + THF, δ) 2.13 (CH₃), 4.86 (CH₂), 5.27 (CH). ¹³C NMR (500 MHz, CDCl₃ + THF, δ) 16.63 (CH₃), 60.64 (CH₂), 68.85 (CH), 169.48 (CO), 207.66 (CO). The chemical shift values for PLGA 20:80 are ¹H NMR δ 2.35 (CH₃), 4.90 (CH₂), 5.39 (CH). ¹³C NMR 16.68 (CH₃), 60.845 (CH₂), 69.30 (CH), 166.459 (CO), 207.44 (CO). Chemical shift values for PLGA 10:90 are ¹H NMR δ 2.34 (CH₃), 4.51 (CH₂), 5.37 (CH). ¹³C NMR 16.11 (CH₃), 61.06 (CH₂), 70.11 (CH), 167.86 (CO), 216.78 (CO). The IR spectrum (S9–S12 Supporting Information) for PLA has characteristic peaks corresponding to OH (3663), CH (2941), CO (1750), and COC (1089). The peaks for PLGA 40:60 are OH (3653), CH (2995), CO (1750), and COC (1088). The peaks for PLGA 20:80 it is OH (3648), CH (2880), CO (1790), and COC (1094). The peaks for PLGA 10:90 are OH (3659), CH (2957), CO (1742), and COC (1086).

The weight average molecular weight of PLA is 8700 Da, and that of copolymers are 9100, 7505, and 8200 for PLGA 40:60, 20:80, and 10:90, respectively. The TGA and DSC thermogram

of these polymers are given in the Supporting Information (S13 and S14) and are tabulated in Table I.

3.2. Characterization of Polymer Blends. The ^1H and ^{13}C NMR chemical shifts (S15–S22 Supporting Information) and IR data of the blends are listed in Table II. The characteristic ^1H NMR spectra of the individual polymers in the blends are expanded and shown in Figure 1. The IR spectra of the four blends are shown in Figure 2. The presence of alcohol OH, lactic acid OH stretch, CH, ester CO (1607), and polycaprolactam amide carbonyl (CO) and secondary amine (NH) in the IR spectra of the blends confirms the presence of all the three polymers.

Figure 3 shows the thermal stability of the polymer blends, and it can be seen that they are stable up to 200 °C. The decomposition temperature of the blends is in the order of USM1 (no appreciable loss until 375 °C) > USM2 (225 °C) > USM3 (200 °C) > USM4 (175 °C). From 375 to 400 °C, there is a weight loss in the range of 77.5, 44.6, 59.7, and 62.05% for USM1, USM2, USM3, and USM4, respectively. There was 14.8% reduction in the weight of USM2 at 620 °C, 11 and 17.2% reduction in the weights of USM3 and USM1, respectively, at 800 °C, and 17.7% reduction in the weight of USM4 at 860 °C. Figure 4 shows the DSC thermogram of the polymeric blends. Sharp melting point peaks at 141.15 and 143.99 °C were observed for USM1 and USM2, respectively. The heat of fusion (ΔH) values for these two blends are 14.26 and 44.34 J/g, respectively. No sharp melting points were observed for USM3 and USM4.

The contact angle of homopolymer PLA and copolymer PLGA are tabulated in Table I ranging from 77 to 51°. But the contact angle of the polymer blends was <5°. The mechanical properties of the homopolymer PLA and copolymer PLGA were poor that even thin films were not possible with the synthesized polymers. The tensile strength of the blends at maximum load is reported in Table II. Blending of PCPL enhanced the film forming ability and also increased the tensile strength and percentage elongation.

3.3. Biocompatibility of Blends. All the blends were compatible with L6 myoblasts cells. Figure 5 shows the confocal laser scanning microscopic images of attached L6 myoblasts on the surface of the four blends after 24 h of incubation. DiI is a live cell dye that stains all viable cells. Such viable cells are observed on the four blended surface. The figure shows bright field image of the cells. The dark spot on the surface represents the cells. More live cells are observed on USM1 than on other blends. USM1 is the most biocompatible material, with more than 95% live cells even at the end of 48 h (Figure 6). But the percentage of viable cells drops down to around 50% with USM4. The cell viability here is determined using MTT assay.

3.4. Hemocompatibility. Figure 7 shows the scanning electron microscopic images of both polymer blends untreated and treated with whole blood. These images when compared with the untreated films reveal that there is no spreading or aggregation of platelets on the surface of the blends which clearly indicates that these blends are hemocompatible (Figure 7). There is no visible formation of thrombus clots on the surface of the polymers but on the contrary there was high protein adsorption. The small group of cells on the surface of USM3 was found to be red blood cells not platelets.

3.5. Encrustation Analysis. The rate of encrustation of Ca, Mg, and P on the surface of the four blends as a function of time is shown in Figure 8–10. Calcium is the predominant

Table II. Characteristic of the Blends

| s. no. | polymer blend | ^1H NMR (ppm) | ^{13}C NMR (ppm) | IR spectra | tensile stress at maximum load (MPa) ^a |
|--------|---------------------------|---|--|--|---|
| 1 | USM1 PLA/PCPL/PVA | 5.63 (s), 5.39 (t, $J = 5$ Hz), 5.29 (q, $J = 10$ Hz), 4.64 (q, $J = 5$ Hz), 4.48 (s), 4.31 (m), 3.98 (m), 2.47 (t, $J = 10$ Hz), 1.46 (m), 1.41 (m), 1.34 (m), 1.30 (m), 0.94 (m). | 212.01, 171.05, 70.20, 70.04, 66.71, 56.32, 38.59, 30.14, 29.64, 28.75, 23.49, 22.77, 15.92, 13.58, 10.48 | OH stretch (3789), NH (3435), CH stretch CO (1733), and amide carbonyl stretch CO (1693) | 0.66 |
| 2 | USM2 PLGA 40:60 /PCPL/PVA | 5.38 (q, $J = 10$ Hz), 4.99 (s), 4.63 (q, $J = 10$ Hz), 4.47 (s), 4.32 (t, $J = 5$ Hz), 2.47 (m), 2.22 (s), 1.74 (m), 1.60 (d, $J = 5$ Hz), 1.46 (m), 1.40 (m), 1.33 (m), 0.93 (m). | 206.21, 177.33, 172.55, 70.23, 67.20, 61.91, 59.65, 38.58, 30.13, 29.62, 28.73, 23.46, 22.74, 18.93, 15.85, 13.50, 10.40 | OH stretch (3780), NH (3453), CH stretch CO (1734), amide carbonyl stretch CO (1685) | 8.82 |
| 3 | USM3 PLGA 20:80 /PCPL/PVA | 5.42 (q, $J = 5$ Hz), 5.01 (s), 4.67 (q, $J = 5$ Hz), 4.51 (s), 4.38 (m), 2.52 (t, $J = 5$ Hz), 1.51 (m), 1.48 (m), 1.36 (m), 0.96 (m) | 209.92, 177.69, 171.98, 70.50, 67.26, 61.83, 59.48, 40.43, 38.61, 30.05, 29.50, 28.65, 23.35, 22.58, 18.48, 13.05, 10.01 | OH stretch (3783), NH (3421), CH stretch CO (1734), and amide carbonyl stretch CO (1687) | 4.75 |
| 4 | USM4 PLGA 10:90 /PCPL/PVA | 5.38 (q, $J = 5$ Hz), 4.99 (s), 4.63 (q, $J = 10$ Hz), 4.47 (s), 4.31 (t, $J = 5$ Hz), 2.35 (s), 2.02 (m), 1.74 (d, $J = 5$ Hz), 1.61 (d, $J = 5$ Hz), 1.46 (m), 1.39 (m), 1.32 (m), 0.93 (m) | 210.00, 177.65, 171.77, 70.15, 67.18, 61.92, 59.72, 53.46, 38.59, 30.15, 28.76, 23.49, 22.78, 19.08, 15.98, 13.82, 10.50 | OH stretch (3522), OH stretch (3723), NH (3472), CH stretch CO (1715), amide carbonyl CO stretch CO (1697) | 5.25 |

^aThe tensile strength of the polycaprolactam used is 16.88 MPa.

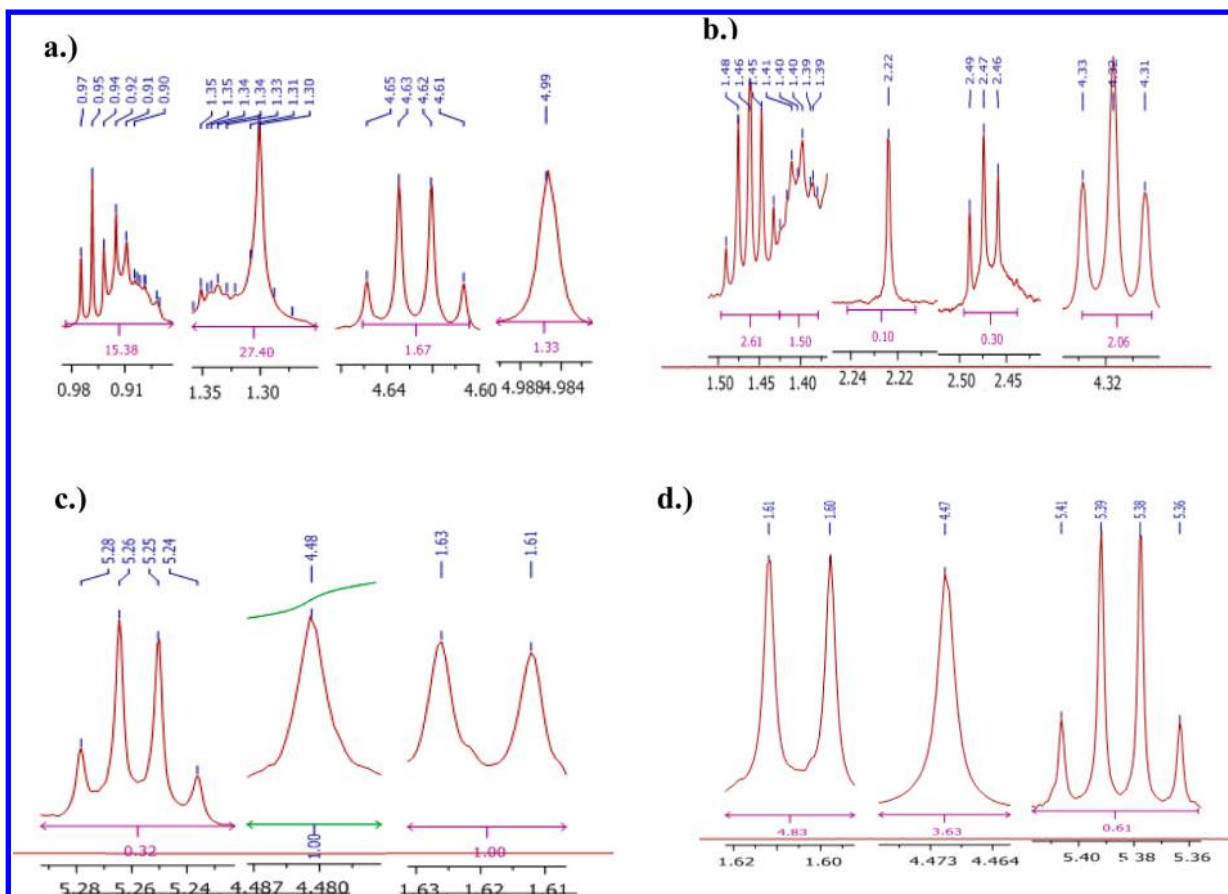


Figure 1. Characteristic expansion ¹H NMR spectrum of (a) PVA, (b) PCPL, (c) PLA, (d) PLGA.

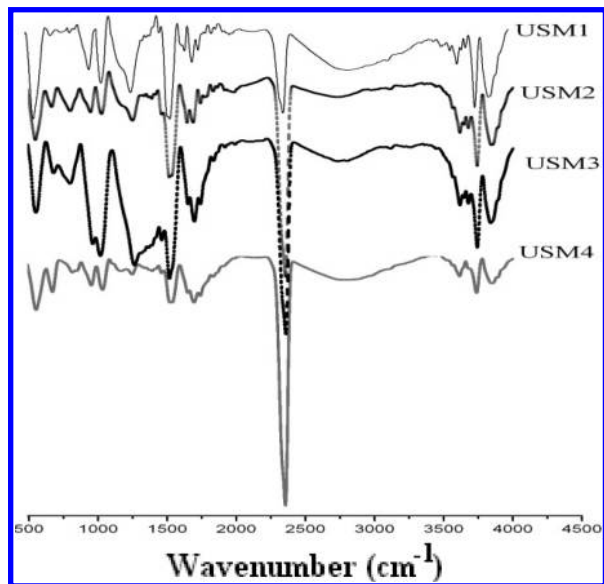


Figure 2. FTIR spectra of blends.

encrustant reaching 80 mg/cm² of the surface in 21 days. This is followed by encrustation of phosphorus (~60 mg/cm² in 21 days) and then magnesium (~16 mg/cm² in 21 days). The pattern of encrustation of salts is similar on all the blends.

3.6. Bacterial Adhesion Analysis. Adhesion of bacteria was higher on blood plasma protein treated blends than on PBS treated ones (Figure 11). Adhesion of *E. coli* is less when compared to *P. mirabilis* on all blends. There is no significant

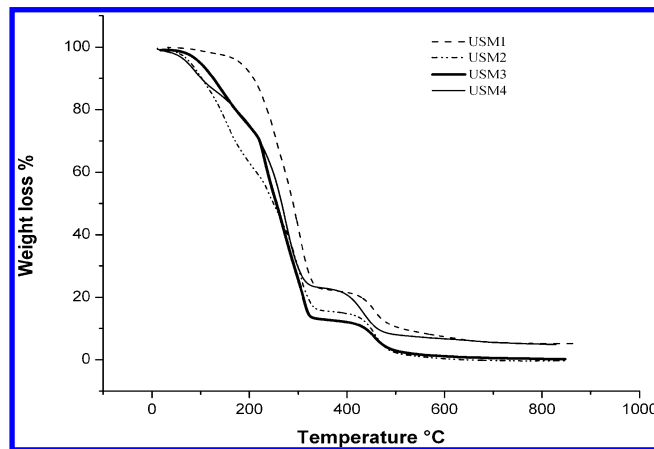


Figure 3. TGA curves of the polymer blend films under N₂ atmosphere at a heating rate of 10 °C min⁻¹.

difference in the extent of adhesion of organisms on these four blends.

3.7. Degradation Analysis. Degradation of the blends was determined by measuring the gravimetric weight loss of the films incubated in artificial urine. At the end of 3 weeks, 3–10% percentage weight loss was observed (Table III). Weight loss was maximum in USM4 and minimum in USM1.

4. DISCUSSION

PLA and PLGA were synthesized by direct melt condensation of the respective monomers in the presence of SnCl₂ at 160 °C.

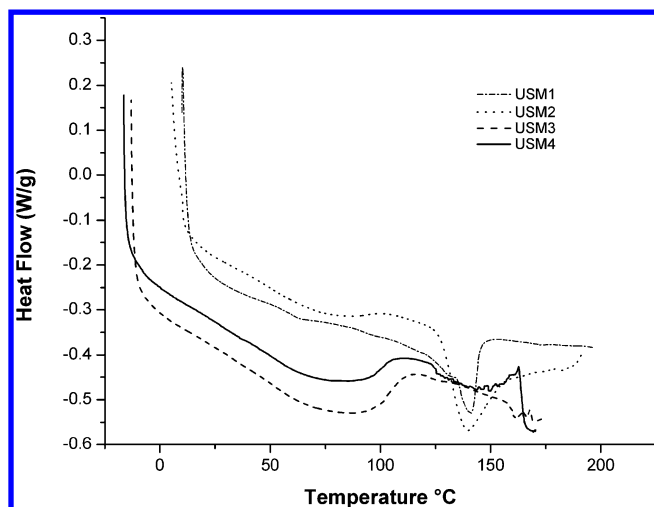


Figure 4. DSC thermograms of polymer blend film at a heating rate of $10\text{ }^{\circ}\text{C min}^{-1}$.

The polymers were characterized by ^1H , ^{13}C NMR, and FTIR spectroscopy. The spectra of these synthesized polymers are consistent with the earlier reports on ring-opening and condensation polymerization of PLA and PLGA.¹⁹ The LA/GA ratios in the PLGA copolymers were all calculated by comparing the ratios of the absorbance at 5.20 (CH) and 4.85 (CH_2) ppm.¹⁹ The homopolymer PLA has low glass transition temperature (T_g). Whereas, the T_g of the copolymer is higher than that of PLA. The increase in the glass transition temperature is mainly due to the increase in the ratio of glycolic acid. The increase in T_g of PLGA when compared to PLA may be due to the increase in the glycolic acid content.²⁰

The IR spectrum of the blends contain characteristics absorption bands for polylactic acid (OH), polyvinyl alcohol (OH),²¹ amide stretching in polycaprolactam (NH),²² indicating the presence of all the three polymers. The presence of three different polymers in the blend is further confirmed by the ^1H and ^{13}C NMR spectra. In the case of polyvinyl alcohol, hydroxyl proton appears at 4.99 ppm as a singlet, two methylene protons as multiplets at 1.35 and 0.97 ppm, and the methine proton at 4.65 ppm. The hydroxyl attached to a

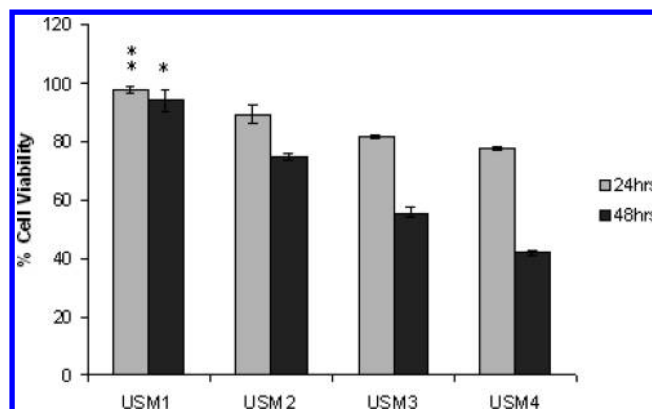


Figure 6. Biocompatibility of polymeric blends. (**) $p < 0.01$ and (*) $p < 0.05$ with respect to other blends.

carbon appears at 70.20 ppm. In the case of polycaprolactam, the nitrogen attached to methylene appears as a triplet at 4.33 ppm, with carbonyl attached to methylene as triplet at 2.49 ppm. The other three methylene peaks appear around 1.48–1.39 ppm as multiplets. The amide carbonyl carbon appears around 206.21, 209.92, and 210.00 ppm. As mentioned earlier, the presence of PLA is confirmed from the methyl proton which appears as doublet around 1.63 ppm, methine proton as quadrate around 5.28 ppm, and the hydroxyl proton as singlet around 4.48 ppm. The acid carbonyl appears around 171.05 ppm. The methyl proton in PLGA appears as doublet at 1.61 ppm, methine proton as quadrate around 5.41 ppm, and methylene proton appear as singlet at 4.47 ppm. The carbonyl in PLA appears around 171.77, 171.98, and 172.55 ppm and that in polyglycolic acid appears around 177.33, 177.65, and 177.69 ppm.¹⁹

Moreover, there is a profound increase in the glass transition temperature of the USM2, 3, and 4 when compared to that of PLA. The increase in the decomposition temperature could be attributed to the relative amount of the individual polymers present which in turn leads to the increase in their thermal behavior.^{23,24}

There is significant increase in the hydrophilicity of the polymer blends when compared to that of homopolymer PLA

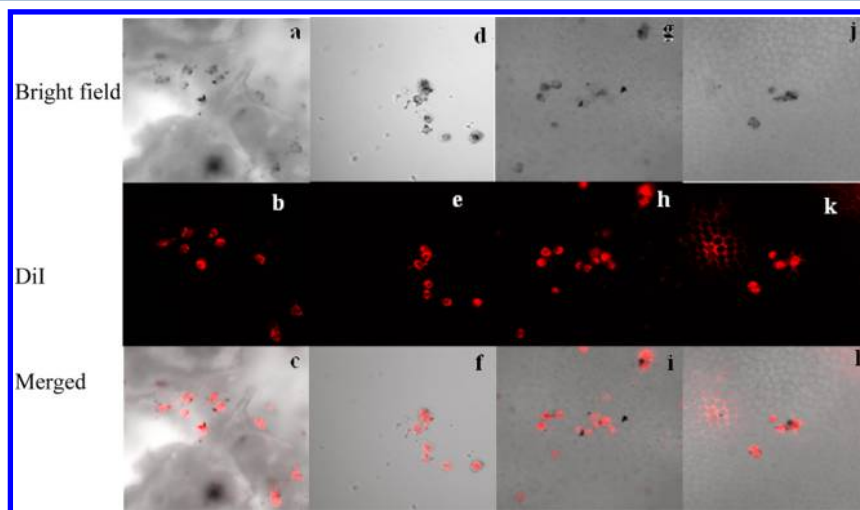


Figure 5. Confocal laser scanning microscopic image of L6 myotubes on the surface of blends after 24 h. The images shows the attachment and growth of cells on USM1 (a–c); USM2 (d–f); USM3 (g–i); and USM4 (j–l).

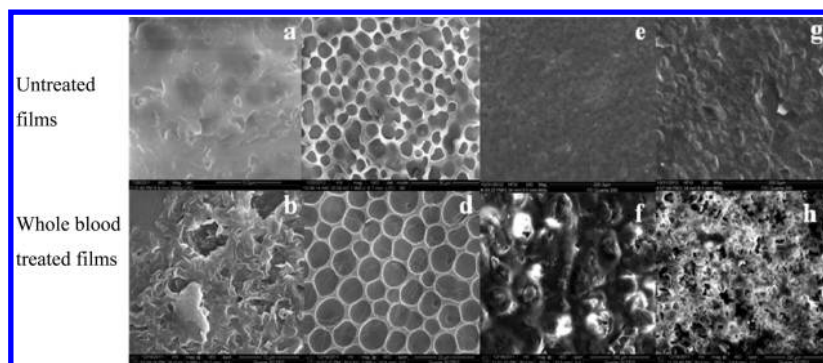


Figure 7. Scanning electron microscopic images of polymeric blends incubated with and without whole blood USM1 (a and b); USM2 (c and d); USM3 (e and f); and USM4 (g and h).

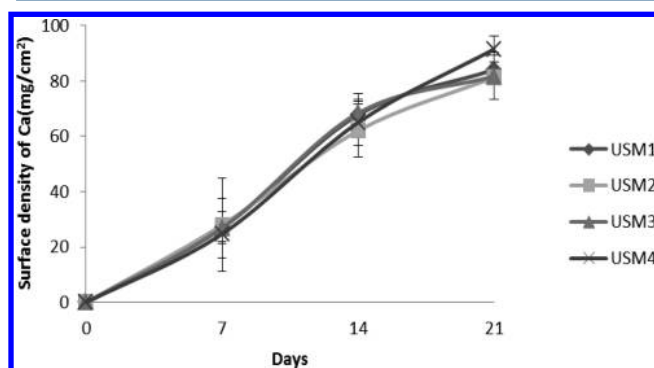


Figure 8. Kinetics of encrustation of calcium on the surface of blends.

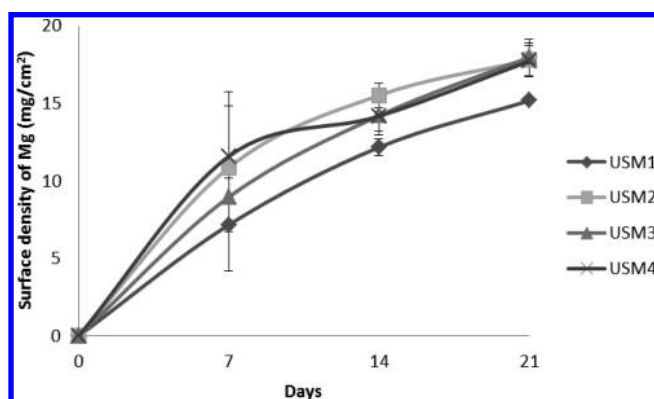


Figure 9. Kinetics of encrustation of magnesium on the surface of blends.

and copolymer PLGA. The blends were extremely made extremely hydrophilic with the addition of PVA with a contact of $<5^\circ$ in all the four blends. Moreover, the mechanical properties of the synthesized polymers were increased significantly by blending with PCPL. The high tensile strength ensures better mechanical strength of the polymer blends than the synthesized the polymer PLA and PLGA (S23–S27, Supporting Information). These values are low compared to the mechanical properties of the commercial polyurethane stents with drainage holes which is around 18 MPa²⁵ which is used currently in clinical practice, but this comparison may be insignificant because ASTM D412 was used to analyze the tensile properties of the polyurethane stents but in our study ASTM D882 was used to study the properties of the thin films which further necessitates a thorough understanding of the

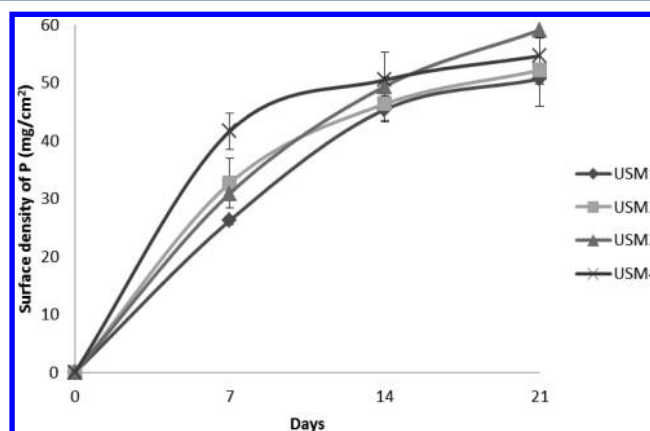


Figure 10. Kinetics of encrustation of phosphorus on the surface of blends.

mechanical property of the polymer blends in molded or die cut form to ensure the use of these blends as a ureteral stent.

USM1 is the most biocompatible which could be attributed to PVA content. PVA imparts hydrophilicity to the blend. Reports have made a clear correlation between the adhesion of fibroblast cells and their proliferation on blends with the amount of PLA content.²⁶ Previous reports indicate that the presence of around 20% of hydrophilic monomers favor good fibroblast adhesion²⁷ with maximum cell growth and spreading observed on moderately hydrophilic polymers having contact angle around 55° .²⁸ In the current study, PVA makes the blends extremely hydrophilic (contact angle $<5^\circ$).

Various attempts to develop a hydrophilic surface for better biocompatibility have been achieved with surface modification. For example, coating with silver nanoparticle¹⁵ increased the biocompatibility of polyaniline surface. Sulfobetaine engineered polymethylmethacrylate (PMMA) decreased fibroblast adhesion when compared to bare polymer.²⁹ Increased cell viability was also observed on polyurethane (PU) coated with hydrophilic macromolecule such as Curdlan³⁰ and bovine serum albumin. Attempts to achieve hydrophilic surface through surface modification had led to increased biocompatibility but in all these cases the bulk property of the polymer was not altered. After surface degradation or erosion of the coating material over a period of time, the bare polymer that is exposed to the body fluids can lead to systemic toxicity. Blends that are biocompatible overcome this problem since they are inherently hydrophilic. Hence the current approach of preparing hydrophilic polymeric blends is more advantageous

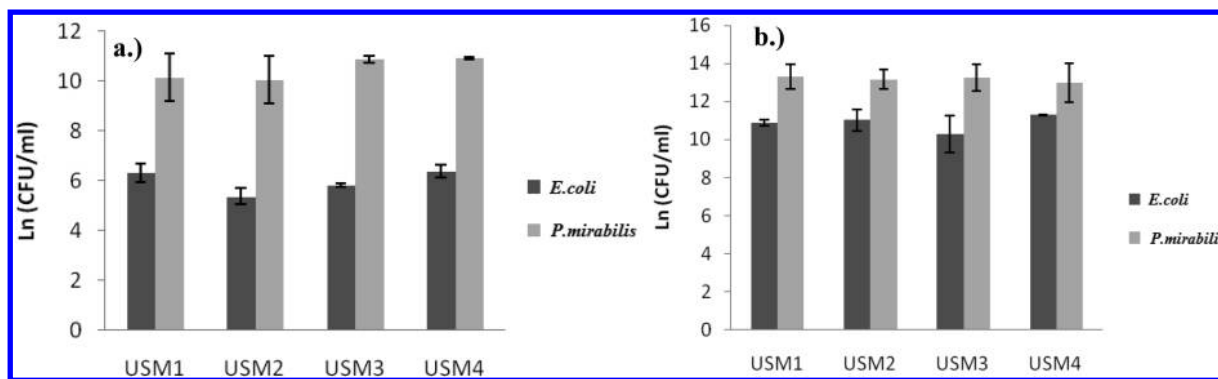


Figure 11. Bacterial adhesion on (a) PBS pretreated and (b) blood plasma pretreated polymer blends.

Table III. Degradation of Polymer Blends in Artificial Urine at the End of Three Weeks

| code | % gravimetric weight loss |
|------|---------------------------|
| USM1 | 3.33 ± 2.90 |
| USM2 | 4.04 ± 2.53 |
| USM3 | 8.67 ± 6.43 |
| USM4 | 10.53 ± 3.29 ^a |

^a*p* < 0.01 with respect to other blends.

than surface modification of polymers to achieve biocompatibility.

Both the platelet adhesion and whole blood *in vitro* assays indicate that these blends are hemocompatible. Moreover increased protein adsorption observed here on the surfaces is mainly due to their hydrophilicity. The type of protein adsorbed has not been investigated in this study, since the adsorption of plasma proteins on material surface has been analyzed in many studies. There is a particular focus on albumin and fibrinogen. The former prevents the adhesion of platelets, and the latter favors platelet adhesion. Albumin adheres well on a hydrophilic surface as fibrinogen does to a hydrophobic surface.³¹ The adsorption of these proteins is governed by electrostatic and hydrophobic interactions. In the case of albumin, they alter their structures so that they overcome all other forces resulting in their adsorption on material surfaces that have same charge as themselves.⁵ Scavenging cells termed as mononuclear phagocytic system (MPS) recognize hydrophobic PLGA. This leads to complement activation, platelet activation, and macrophage interactions.³² But in the present case, this is overcome by the addition of PVA which is very hydrophilic. Earlier attempts to increase the hemocompatibility of different polymers including polycaprolactone by incorporating biomacromolecules resulted in significant reduction in the platelet adhesion and spreading.¹⁶ But as discussed earlier, surface engineering can solve the issue only for a short period of time, following which the exposure of bare polymer surface to blood may result in the adhesion of activated monocytes. The current study has identified a good hemocompatible material with no activation and adhesion of monocytes.

Calcium was the predominant encrustant (~80 mg/cm²) at the end of 3 weeks. Earlier studies on polyurethane surface¹ also indicated that calcium was the predominant encrustant. Encrustation of magnesium on the blends observed here was similar to that observed on polyurethane surface. The adhesion of phosphorus on these blends was very less when compared to the encrustation on polyurethane.

In general hydrogels and hydrophilic materials possess several properties including lubricity, biocompatibility, and resistance to encrustation and bacterial adhesion.³³ Earlier studies also show that deposition of struvite and hydroxyapatite, the two predominant encrustants in the urinary tract environment, are significantly less on hydrophilic poly-(vinylpyrrolidone–iodine) engineered polyurethane surface.³³ Polyurethane and modified PU are more widely investigated since they give satisfactory results at least for a short period of time.² Encrustation of salts on polymer surface is influenced by three important factors (i) composition of the organic layer adhered, (ii) properties of the adhering bacteria, and (iii) the composition of the urinary salts. In the present study with artificial urine, there was significant reduction in the pattern of encrustation of magnesium and phosphorus when compared to the PU.¹ This could be attributed to the hydrophilicity of the blend, as previous studies have also shown that a hydrophilic surface will resist encrustation *in vivo*.^{34,35}

The surface property of the bacteria plays an important role in its adhesion to the polymer surface. In the present study *E. coli* adheres less than *P. mirabilis* probably because the former is relatively hydrophobic than *P. mirabilis*. The adhesion was more in the presence of blood plasma proteins than on PBS treated ones. This may be due to the fact that the adhered proteins alter the hydrophilicity of the surface. The current study supports the literature findings that increased hydrophilicity resists bacterial attachment.^{4,15,36}

Degradation of the blends begins with the degradation of the PLA and PLGA content. Degradation of lactic and glycolic acid occurs in four consecutive steps which includes hydration, initial degradation, final degradation, and solubilization.³⁷ There was a considerable weight loss in the blends USM3 and 4, with maximum weight loss observed in USM4 (10.5%) in 3 weeks. The composition of the blends influences the hydrophilicity and the wettability and also influences the hydration of the blends.³⁸ In the current study the order of degradation of these blends are proportional to the glycolic acid content in them. SEM and visual observations indicate that the integrity of the films is not lost till the end of 3 weeks. This is line with earlier findings that, only with a considerable loss in the molecular weight of the polymers, there is a reduction in its mechanical strength but the material still maintains its integrity.³⁸

5. CONCLUSION

Low molecular weight homopolymer, PLA, and copolymer, PLGA, were synthesized and characterized. Novel hydrophilic blends were prepared with PLGA, PCPL, and PVA and characterized with IR and NMR to confirm their presence. The

mechanical stability of the polymer blends were also analyzed with tensile strength analyzer. The biocompatibility and hemocompatibility of all the blends were determined with whole blood and MTT assay. After 48 h of incubation, 50–94% cells were viable with all the blends after 48 h of incubation. The blends investigated for ureteral application indicates a significant reduction in the adhesion of uropathogens. The adhesion of *E. coli* was much less when compared to *P. mirabilis*. Adhesion of organism was similar on all the blends. Calcium was the predominant encrustant on all the blends with a significant reduction in magnesium and phosphorus. Maximum weight loss was observed with USM4 (10.8%) in 3 weeks, and minimum, with USM1 (3%). But USM1 is more biocompatible (with 95% cell viability) than USM4. Hence it can be concluded that each of the four blends are biodegradable and appropriate for ureteral application with polylactic acid based blend (USM1) dominating other blends in all aspects.

However, more detailed investigations are necessary to understand the effect of molecular weight on the degradation pattern. Although, L6 myoblasts cells were used in the current study, further investigations need to be carried out with different fibroblast cell lines. Whole blood studies were performed with blood samples from the same set of healthy human volunteers. Detailed studies with different blood groups from different individuals would further validate the hemocompatibility of these blends. Only *E. coli* and *P. mirabilis* were included in the study because they are of urological importance, but ureteral stents are also colonized by many other Gram negative bacteria. So a thorough understanding of the role of other bacteria on the surface of the blends in combination with protein needs to be investigated for longer duration. In vivo biocompatibility and encrustation analysis is necessary to validate the blends for their application as ureteral stent in human.

■ ASSOCIATED CONTENT

● Supporting Information

S1–S8 as described in text ¹H and ¹³C NMR spectra, S9–S12 the IR spectra, and S13–S14 thermal analysis TGA and DSC of synthesized polymers. S15–S22 complete ¹H and ¹³C NMR characterization of the polymeric blends. S23–S27 complete tensile strength analysis of the polymer blends and polycaprolactam. This information is available free of charge via the Internet at <http://pubs.acs.org/>.

■ AUTHOR INFORMATION

Corresponding Author

*E-mail: mukeshd@iitm.ac.in. Phone: +914422574107.

Notes

The authors declare no competing financial interest.

■ ACKNOWLEDGMENTS

The authors thank Sophisticated Analytical Instrumentation Facility (SAIF), Department of Chemistry, and Department of Metallurgical and Materials Engineering, IIT Madras, for analytical support. The authors also thank Dr. Vinodhini Sridharan, Assistant Professor, Department of Pharmacology, SRM Dental College, India, for her help in microbiological analysis.

■ REFERENCES

- (1) Venkatesan, N.; Shroff, S.; Jeyachandran, K.; Doble, M. Effect of uropathogens on in vitro encrustation of polyurethane double J ureteral stents. *Urol. Res.* **2011**, *39*, 29.
- (2) Venkatesan, N.; Shroff, S.; Jayachandran, K.; Doble, M. Polymers as ureteral stents. *J. Endourol.* **2010**, *24*, 191.
- (3) Santin, M.; Motta, A.; Denyer, S. P.; Cannas, M. Effect of the urine conditioning film on ureteral stent encrustation and characterization of its protein composition. *Biomaterials* **1999**, *20*, 1245.
- (4) Cunliffe, D.; Smart, C. A.; Alexander, C.; Vulfson, E. N. Bacterial adhesion at synthetic surfaces. *Appl. Environ. Microbiol.* **1999**, *65*, 4995.
- (5) Norde, W.; Lyklema, J. Protein adsorption and bacterial adhesion to solid surfaces: a colloid-chemical approach. *Colloids Surf.* **1989**, *38*, 1.
- (6) Lumiaho, J.; Heino, A.; Kauppinen, T.; Talja, M.; Alhava, E.; Valimaa, T.; Tarmala, P. Drainage and antireflux characteristics of a biodegradable self-reinforced, self-expanding X-ray-positive poly-L, D-lactide spiral partial ureteral stent: an experimental study. *J. Endourol.* **2007**, *21*, 1559.
- (7) Petas, A.; Vuopio-Varkila, J.; Siitonen, A.; Valimaa, T.; Talja, M.; Taari, K. Bacterial adherence to self-reinforced polyglycolic acid and self-reinforced polylactic acid 96 urological spiral stents in vitro. *Biomaterials* **1998**, *19*, 677.
- (8) Lumiaho, J.; Heino, A.; Aaltomaa, S.; Valimaa, T.; Talja, M. A short biodegradable helical spiral ureteric stent provides better antireflux and drainage properties than a double-J stent. *Scand. J. Urol. Nephrol.* **2011**, *1*.
- (9) Kotsar, A.; Isotalo, T.; Mikkonen, J.; Juuti, H.; Martikainen, P. M.; Talja, M.; Kellomaki, M.; Tormala, P.; Tammela, T. L. J. A new biodegradable braided self-expandable PLGA prostatic stent: an experimental study in the rabbit. *J. Endourol.* **2008**, *22*, 1065.
- (10) Talja, M.; Multanen, M.; Valimaa, T.; Tormala, P. Bioabsorbable SR-PLGA horn stent after antegrade endopyelotomy: a case report. *J. Endourol.* **2002**, *16*, 299.
- (11) Kehinde, E. O.; Rotimi, V. O.; Al-Hunayan, A.; Abdul-Halim, H.; Boland, F.; Al-Awadi, K. A. Bacteriology of urinary tract infection associated with indwelling J ureteral stents. *J. Endourol.* **2004**, *18*, 891.
- (12) Clapham, L.; McLean, R. J. C.; Nickel, J. C.; Downey, J.; Costerton, J. W. The influence of bacteria on struvite crystal habit and its importance in urinary stone formation. *J. Cryst. Growth* **1990**, *104*, 475.
- (13) Lan, P.; Zhang, Y.; Gao, Q.; Shao, H.; Hu, X. Studies on the synthesis and thermal properties of copoly (lactic acid/glycolic acid) by direct melt polycondensation. *J. Appl. Polym. Sci.* **2004**, *92*, 2163.
- (14) Wang, L.; Zhang, Z.; Chen, H.; Zhang, S.; Xiong, C. Preparation and characterization of biodegradable thermoplastic Elastomers (PLCA/PLGA blends). *J. Polym. Res.* **2010**, *17*, 77.
- (15) Prabhakar, P. K.; Raj, S.; Sawant, S. N.; Doble, M. Biocompatibility studies on polyaniline and polyaniline-silver nanoparticle coated polyurethane composite. *Colloids Surf. B.* **2011**, *86*, 146.
- (16) Khandwekar, A. P.; Patil, D. P.; Shouche, Y.; Doble, M. Surface Engineering of Polycaprolactone by Biomacromolecules and their Blood Compatibility. *J. Biomater. Appl.* **2011**, *26*, 227.
- (17) Hogt, A. H.; Dankert, J.; Feijen, J. A. N. Adhesion of *Staphylococcus epidermidis* and *Staphylococcus saprophyticus* to a hydrophobic biomaterial. *J. Gen. Microbiol.* **1985**, *131*, 2485.
- (18) Deniz, G. Synthesis, characterization and in vitro degradation of poly (DL-lactide)/poly (DL-lactide-co-glycolide) films. *Turk. J. Chem.* **1999**, *23*, 153.
- (19) Gilding, D. K.; Reed, A. M. Biodegradable polymers for use in surgery—polyglycolic/poly (actic acid) homo-and copolymers: 1. *Polymer* **1979**, *20*, 1459.
- (20) Zhou, S.; Deng, X.; Li, X.; Jia, W.; Liu, L. Synthesis and characterization of biodegradable low molecular weight aliphatic polyesters and their use in protein delivery systems. *J. Appl. Polym. Sci.* **2004**, *91*, 1848.
- (21) Krimm, S.; Liang, C. Y.; Sutherland, G. Infrared spectra of high polymers. V. Polyvinyl alcohol. *J. Polym. Sci.* **1956**, *22*, 227.

(22) Frayer, P. D.; Koenig, J. L.; Lando, J. B. Infrared studies of chain folding in polymers. X. polycaprolactam. *J. Macromol. Sci. B Physics* **1972**, *6*, 129.

(23) Coleman, M. M.; Graf, J. F.; Painter, P. C. *Specific interactions and the miscibility of polymer blends: practical guides for predicting & designing miscible polymer mixtures*; Technomic Publishing Co.: Lancaster, PA, 1991.

(24) Lu, X.; Weiss, R. A. Relationship between the glass transition temperature and the interaction parameter of miscible binary polymer blends. *Macromolecules* **1992**, *25*, 3242.

(25) Gorman, S. P.; Jones, D. S.; Bonner, M. C.; Akay, M.; Keane, P. F. Mechanical performance of polyurethane ureteral stents in vitro and ex vivo. *Biomaterials* **1997**, *18*, 1379.

(26) Watanabe, J.; Ishihara, K. Change in cell adhesion property on cytocompatible interface using phospholipid polymer grafted with poly(D,L-lactic acid) segment for tissue engineering. *Sci. Technol. Adv. Mat.* **2003**, *4*, 539.

(27) Campillo-Fernandez, A. J.; Unger, R. E.; Peters, K.; Halstenberg, S.; Santos, M.; Sanchez, M. S.; Dueas, J. M. M.; Pradas, M. M.; Ribelles, J. L. G.; Kirkpatrick, C. J. Analysis of the biological response of endothelial and fibroblast cells cultured on synthetic scaffolds with various hydrophilic/hydrophobic ratios: influence of fibronectin adsorption and conformation. *Tissue Eng. A* **2008**, *15*, 1331.

(28) Khang, G.; Lee, S. J.; Lee, J. H.; Kim, Y. S.; Lee, H. B. Interaction of fibroblast cells on poly (lactide-co-glycolide) surface with wettability chemogradient. *Biomed. Mater. Eng.* **1999**, *9*, 179.

(29) Khandwekar, A. P.; Patil, D. P.; Shouche, Y. S.; Doble, M. The biocompatibility of sulfobetaine engineered polymethylmethacrylate by surface entrapment technique. *J. Mater. Sci. Mater. Med.* **2010**, *21*, 635.

(30) Khandwekar, A. P.; Patil, D. P.; Khandwekar, V.; Shouche, Y. S.; Sawant, S.; Doble, M. TecoflexTM functionalization by Curdlan and its effect on protein adsorption and bacterial and tissue cell adhesion. *J. Mater. Sci. Mater. Med.* **2009**, *20*, 1115.

(31) Klee, D.; Höcker, H. Polymers for biomedical applications: improvement of the interface compatibility. *Biomed. Appl. Polymer Blends* **1999**, *1*.

(32) Thasneem, Y. M.; Sajeesh, S.; Sharma, C. P. Effect of thiol functionalization on the hemocompatibility of PLGA nanoparticles. *J. Biomed. Mater. Res. A* **2011**, *99*, 607.

(33) Khandwekar, A. P.; Doble, M. Physicochemical characterisation and biological evaluation of polyvinylpyrrolidone-iodine engineered polyurethane (Tecoflex^Å). *J. Mater. Sci. Mater. Med.* **2011**, *1*.

(34) Holmes, S. A. V.; Cheng, C.; Whitfield, H. N. The development of synthetic polymers that resist encrustation on exposure to urine. *Brit. J. Urol.* **1992**, *69*, 651.

(35) Miller, J. M. The effect of Hydron on latex urinary catheters. *J. Urol.* **1975**, *113*, 530.

(36) Veluchamy, P.; Sivakumar, P. M.; Doble, M. Immobilization of subtilisin on polycaprolactam for antimicrobial food packaging applications. *J. Agricult. Food. Chem.* **2011**, *59*, 10869.

(37) Kumar, G. S. *Biodegradable polymers: prospects and progress*; Marcel Dekker Inc: New York and Basel, 1987.

(38) Wu, X. S.; Wang, N. Synthesis, characterization, biodegradation, and drug delivery application of biodegradable lactic/glycolic acid polymers. Part II: biodegradation. *J. Biomater. Sci., Polym. Ed.* **2001**, *12*, 21.